

Computer Simulation of Vibration Robot Created for the Wall Movement

¹Jamil Al-Azzeh, ²S.F. Yatsun, ²A.A. Cherepanov,
²I.V. Lupehina and ²V.S. Dichenko
¹Al'Balqa Applied University, Arsalt, Jordan
²Southwest State University, Chengqing, China

Abstract: Current research devoted to the question of mechanical vibration system simulation. The model created taken into account the dry friction force which provides the movement of a mobile object (vibrobot) on the vertical surface. Computer simulation provided in current study shows that the most effective and non-energy-intensive method of robot movement control is the regulation of phase difference of unbalanced units rotation.

Key words: Robots, vibration control, numerical simulation, computer, energy

INTRODUCTION

Wheel, carterpillar, step and colubrine systems are usually used as a propeller of mobile robots movement (Bolotnik *et al.*, 2006a, b; Yatsun *et al.*, 2008). To create forces of adhesive bond with a surface they use the systems of pneumomatic suction caps installed on a robot body and its agile parts the action of which is based on the vacuum between an outer surface and a contact surface of suction caps. There are passive ones which create the lowered pressure between the adjoined surfaces within the contact and active ones which provide the continuous air exhaust from the suction cap. The lack of gaps within the contact with the surface what makes robot movements difficult on uneven surfaces is the best condition of a good bond with a surface of a device supplied with the passive pneumosystem. This drawback is removed in active pneumosystems which thanks to the constant air exhaust helps a robot to be on the surface even at gap presence (Chernousko *et al.*, 2005).

The other way of adhesive forces creation is the use of sticking items the lack of which is the fast grit leading to the bond reduction. Recently the systems of bond forces based on the use of special unique basic robot surfaces supplied by nanofibers have become popular. There are works showing us the opportunities of using sharp needle like surfaces which also allow the robot to be on the vertical surface.

The common drawback is the robot has a contact with the surface which is significantly smaller than its body what reduces the reliability of its fixing on the vertical surface (Chashchukhin, 2008; Sooraksa and Chen, 1998). To raise the effectiveness the opportunity of using

the whole body to organize the distributed contact with the surface is studied in this research. It is obvious this way allows to significantly raise the robot reliability to be fixed on the vertical wall and reduces the requirements to the elements which provide the local point contact.

THE ROBOT DESCRIPTION (THE MATHEMATICAL MODEL)

Let us study a mobile robot created for movement along the vertical surface which has a whole body contact with it. The scheme of the robot is given (Fig. 1).

The robot consists of a body 1 which has a rectangular parallelepiped form. Within the body two pairs of unbalanced units 2 and 3 creating horizontal and vertical harmonic conditions are fastened. It is

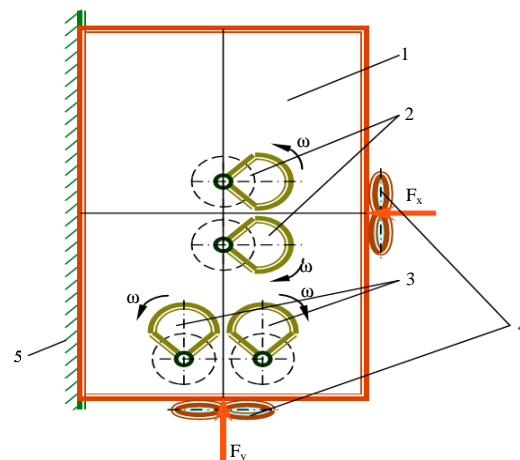


Fig. 1: The scheme of the robot

accomplished by the in-phase rotation of each pair of unbalanced units in opposite directions. The angular velocity in each pair is ω . The fans 4 create constant efforts of pressing to the surface 5 and the robot lifting. The robot mechanism is when the resultant influence of a couple of unbalanced units and the fans are directed along the body symmetry axis. In the Fig. 1, vectors F_x and F_y mean these total impact. Obviously, the given forces are:

$$F_x = P_x + A_x \sin(\omega t) \quad (1)$$

$$F_y = P_y + A_y \sin(\omega t + \varphi) \quad (2)$$

Where:

- P_x, P_y = Constant forces created by the fans
- A_x, A_y = Amplitudes of the forces generated by unbalanced units which generally do not equal to each other
- φ = Phase difference in harmonic forces created by unbalanced units

Making the mathematical model let us ignore the fluctuations of the center position of mass contracture, reckoning it is situated in the centre of the body symmetry. Figure 2 illustrates the designing scheme. At the scheme parameters L_x, L_y are geometrical dimensions of body sections.

Except F_x and F_y forces the gravity mg also has its power to the studied system from the surface side-the force of Coulomb friction F_{fr} and normal reaction N . The equation of movement along the surface is the following:

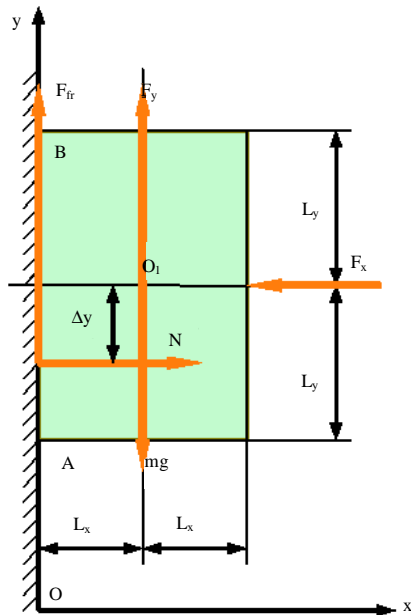


Fig. 2: The design scheme of the forces acting at the robot

$$m\ddot{y} = F_{fr} + F_y - mg \quad (3)$$

Where friction force is given in the form of a piecewise continuous analytical model:

$$F_{fr} = \begin{cases} -k \cdot N \cdot \text{sign}(\dot{y}), & \dot{y} \neq 0 \\ -F_0 = -(F_y - mg), & \dot{y} = 0, |F_0| \leq k \cdot N \\ -k \cdot N \cdot \text{sign}(F_0), & \dot{y} = 0, |F_0| > k \cdot N \end{cases} \quad (4)$$

Where:

- F_0 = Projection to Y-axis of the resultant force of all forces applied to robot mechanism expect friction force
- k = Friction coefficient
- \dot{y} = Robot speed along Y-axis

As the robot moves along the vertical surface, the pressing force F_x is balanced by the normal reaction. But within this movement the normal reaction must be positive. It limits the efforts created by the fan and unbalanced units, precisely for the constant performance of inequality $F_x = P_x + A_x \sin(\omega t) > 0$ it is necessary to observe the conditions for amplitude and modules of the constant force:

$$P_x > A_x \quad (5)$$

Thus, the inequality is the condition of continuous (unseparated) movement along the vertical surface. Nevertheless its fulfillment does not guarantee the pressing of all body verges and here is the explanation of it. Both friction force and normal reaction of surfaces are the forces distributed on contact area. The intensity $n(y)$ of normal reaction can have only non-negative values because there is no adherence and the distribution picture is represented according to Fig. 3.

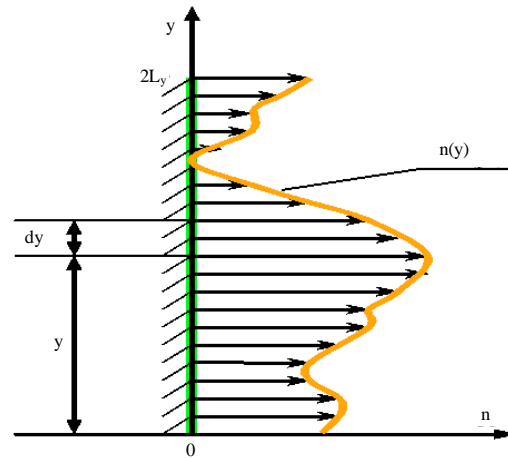


Fig. 3: The distribution scheme of normal reaction of surfaces

Let us show that the resultant force of such loading cannot have the resultant force at the extreme points. The algebraic moment of loading to point O equals to the integral:

$$M_0(N) = - \int_0^{2L_y} n(y)ydy$$

while as $n(y), y \geq 0$, the moment of the resultant force is negative and therefore its contact point is higher than zero. If the contact point is the extreme upper point of loading, the difference between the moment of estimated resultant force and the moment of loading equals to:

$$-N \cdot 2L_y + \int_0^{2L_y} n(y)ydy = \int_0^{2L_y} n(y)(2L_y - y)dy > 0$$

i.e., the loading moment module is smaller than the module of estimated resultant force the contact point of which should be below the extreme high one. As a result it is clear that the resultant force of the distributed normal force is situated strictly between the extreme points. If the resultant force is affixed to for example, the point O, researchers can see that the inequality:

$$\int_0^{2L_y} n(y)ydy = 0$$

is fulfilled what is possible when the intensity is $n(y) = 0$ for all points except $y = 0$. The same happens when the difference of resultant force moment equals to 0 being affixed to the upper point and the loading moment it is obvious that the intensity must be equal to zero at all points, except the upper one. But then it is clear the robot body separates from the wall and starts to rotate around one of the extreme points what means that the progressive movement is being broken and the robot complete detachment from the wall can take place.

Let us find out the limits of system parameters where the detachment doesn't happen neither at movements nor at rest conditions researchers should make an equation of the moments of the body gravity center points O_1 (Fig. 2). The level arm Δy of normal reaction N must be within the interval $(-L_y, L_y)$ where L_y is a half length of the body. The equation of the moments at rest moments and adherence cases is the following:

$$N\Delta y - F_g L_x = 0 \tag{6}$$

If the robot moves, taken into consideration the friction module Eq. 4, the level arm reaction will be determined by the body width and the friction coefficient:

$$\Delta y = k \cdot \text{sign}(\dot{y}) L_x$$

while the attached point N is displaced from the center to the side of movement. It is obvious the robot geometrical parameters for turning exclusion must be equal to the following equation:

$$\frac{L_y}{L_x} > k \tag{7}$$

In the bound case when, $L_y/L_x = k$, the body at the movement begins to trip turning around the front supporting point. But the width must be more than the supporting length at 10 times (if the friction coefficient is $k = 0, 1$)! In practice the length and the width of the contact square of the similar mechanism providing the stability of the progressive movement along the surface of any incline must overcome the height.

At rest moment friction force as we can see from Eq. 3 and 4, equals to $F_{fr} = mg - F_y = mg - P_y - A_y \sin(\omega t + \varphi)$. But $N = F_x = P_x + A_x$. Then to prevent the detachment there is a double inequality:

$$\begin{aligned} -L_y (P_x + A_x \text{sign} \omega t) < L_x (mg - P_y - A_y \text{sign}(\omega t + \varphi)) \\ < L_y (P_x + A_x \text{sign} \omega t) \end{aligned} \tag{8}$$

But the restriction of the friction module at balance has another double inequality:

$$\begin{aligned} -k(P_x + A_x \text{sign} \omega t) < mg - P_y - A_y \text{sign}(\omega t + \varphi) \\ < k(P_x + A_x \text{sign} \omega t) \end{aligned} \tag{9}$$

What determines the parameter field being a subset of the field in the inequality (Eq. 8). It is easy to prove dividing (Eq. 8) into the positive value L_x and taking into account the condition (Eq. 7). Then, the fulfillment of (Eq. 8) is made from the fulfillment at peace state (Eq. 9) researchers come to the conclusion that at adherence absence the robot cannot begin the rotation around its extreme point.

The algorithm of integration of differential equations and results of numerical simulation: To integrate the systems of differential equations the integrated algorithm based on Euler Method (Gear and Petzold, 1984) was used. The algorithm represented in the Fig. 4. Before using the algorithm the user feedings in the values of the system parameters which determine its behavior and operating condition and also the integrated parameters: discreteness, integrated time, etc.

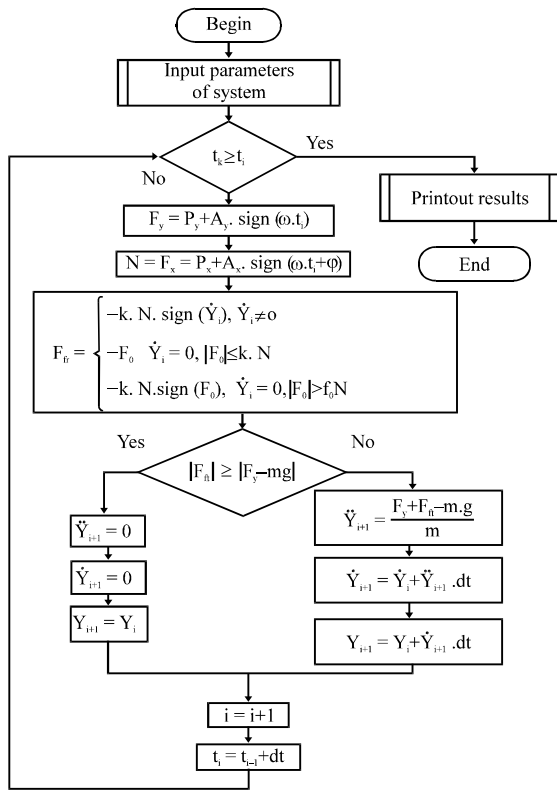


Fig. 4: The algorithm of the numerical integration of the differential equations based on Euler Method

After that the thread of program in the loop with the “while” type at the condition of which the current meaning of the time variable is compared to the integrated time. If the current meaning of the time variable exceeds the integrated time, the outlet of the cycle takes place if no, the differential equations are integrated on the next time step. At the given algorithm the movement using the friction dry module reckoning the peace friction is simulated. The condition “more-equal” of friction force should be checked to the rest external forces. If friction force is more or equals to the total sum of the rest external forces, variables of coordinates has the value calculated at the previous integrated step is assigned to the X-axis, the variables of acceleration and speed are reset at the next step. In case the friction force is smaller than the sum of the rest external forces, the solution of the vertical projection of the movement system takes place using Euler Method. After computation of acceleration, speed and coordinates for the next step of integration the time variable is increasing and the algorithm is checking the integration time.

The dependence of the influence of the constant component P_y to the vibrobot movements along the vertical surface is examined at the constant meanings of

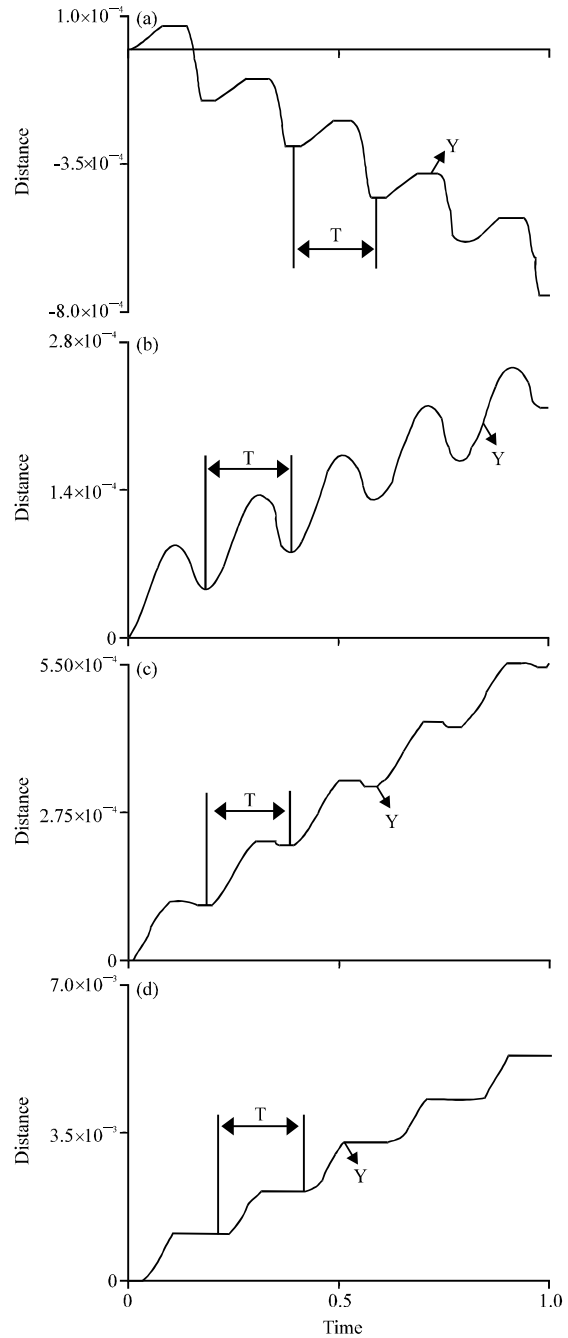


Fig. 5: The relation between time and distance of vertical robot movement computed using different values of the P_y parameter: a) $P_y = 3.1$; b) $P_y = 3.3$; c) $P_y = 3.1$ and d) $P_y = 3.9$

the rest parameters (Fig. 5). Final results of simulation represented as: $k = 0.6$ $\omega = 5$ (Hz) $m = 0.3$ (kg) $P_x = 2$ (N) $A_x = 1$ (N) $A_y = 1$ (N) $\phi = 0$ (Rad).

The analysis of the schemes of the mobile unit movement shows that the ascent height has a significant

dependency on the constant component of the vertical force of robot body lifting. At the increasing of the constant component of 3.8 Newtons the robot begins to move without sliding from the inclined surface. At the reduction of the 3.1 Newton the mechanism stops moving

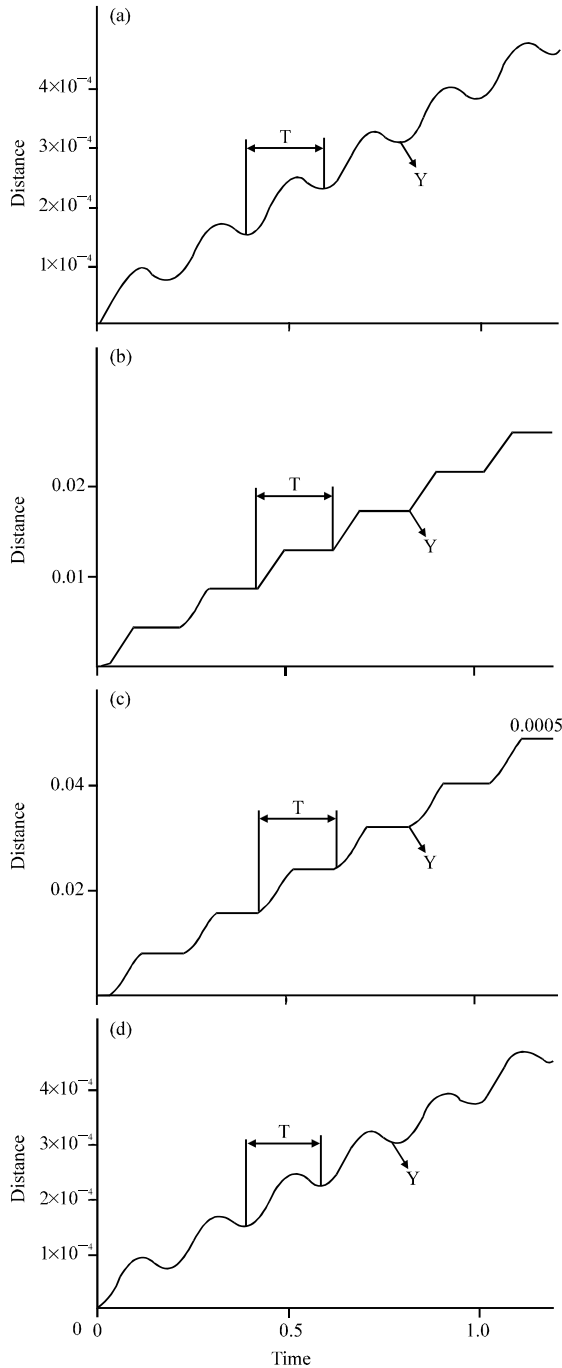


Fig. 6: The relation between time and distance of vertical robot movement computed using different values of the φ parameter. a) $Q = 2\pi \cdot 0.2$; b) $Q = 2\pi \cdot 0.7$; c) $Q = 2\pi \cdot 0.5$ and d) $Q = 2\pi \cdot 0.9$

along the vertical wall and the periodic falling of the mechanism happens. The middle falling speed remains unchangeable. Further, research discovers relation between phase difference harmonic forces and vibrobot movement on vertical surfaces (Fig. 6). During simulation following parameters has been detected: $k = 0.6$ $\omega = 5$ (Hz) $m = 0.3$ (kg) $A_x = 1$ (N) $A_y = 1$ (N) $P_y = 3.4$ (N) $P_x = 2$ (N).

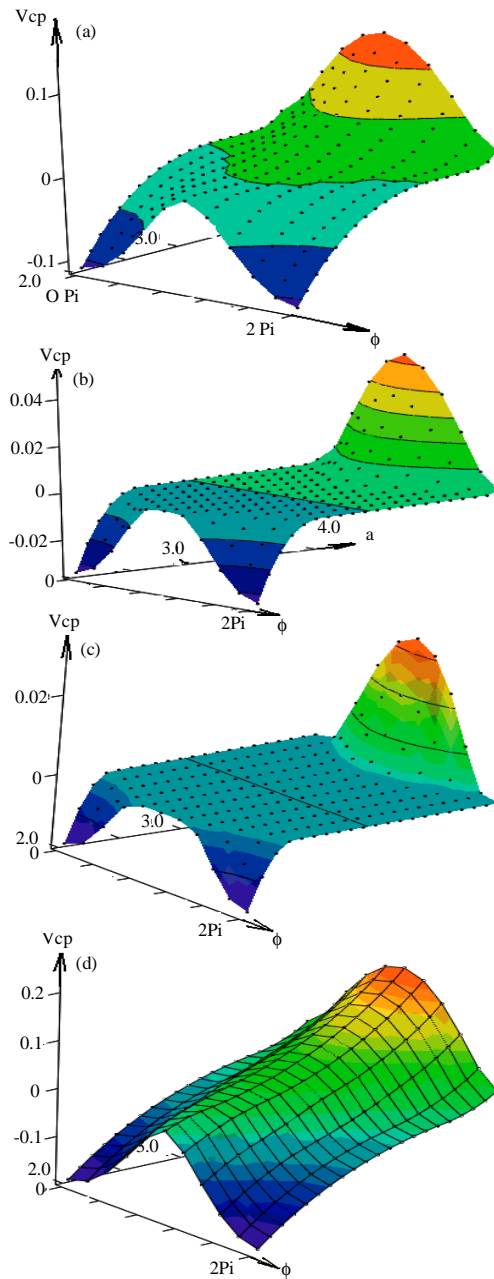


Fig. 7: The dependency graph of the average speed of the vertical lifting on the phase angle and the lifting power. a) $A_x = 1, A_y = 1$; b) $A_x = 0.5, A_y = 0.5$; c) $A_x = 0.5, A_y = 0.3$ and d) $A_x = 1.5, A_y = 1.5$

The studies of system behavior at different values of the phase difference between two harmonic conditions generated by two pairs of unbalanced units show that even at the values of drawing-in efforts which do not provide the operating time without sliding from the vertical surface this regime can be provided. At the given schemes it is distinctly seen the maximum movement speed without sliding is provided at the phase difference near π (180°).

The research has showed that these two parameters have more significant impact to the mechanism of the movement system and particularly to the middle speed of the movement system. The further research of the behavior was conducted with the help of the linear approximation of the differential equations solution (linear approximation of solution of differential equation) and 3D graphs creation (Fig. 7). The modeling was conducted at the following conditions: $k = 0.6$ $\omega = 5$ (Hz) $m = 0.3$ (kg) $P_x = 2$ (H) $P_y \in [2.0; 4.0]$ (H), $\varphi \in [0; 2\pi]$ radians.

CONCLUSION

The creation of vibrobots for vertical surface movements is one of the possible ways of improving the vibromovement principle, increasing the vibrobot mobility. The mechanism and the average movement speed are determined by the parameter set. The most effective and non-energy-intensive method of control is the regulation of phase difference of unbalanced units rotation. At the similar value of the constant component of the vertical force and at different values of phase difference the

maximum speed value is seen at $\varphi = \pi$. The given maximum at $\varphi = \pi$ is seen at 3D curves in the form of the hump passing through the whole surface.

REFERENCES

- Bolotnik, N., I. Zeidis, K. Cimmerman and S.F. Yatsyn, 2006a. Dynamics of controlled movements of vibration systems. Russian Acad. Sci., 5: 1-11.
- Bolotnik, N.N., S.F. Jatsun, A.S. Jatsun and A.A. Cherepanov, 2006b. Automatically controlled vibration-driven robots. Proceedings of the IEEE International Conference on Mechatronics, July 3-5, 2006, Budapest, pp: 438-441.
- Chashchukhin, V.G., 2008. Simulation of dynamics and determination of control parameters of inpipe minirobot. J. Comput. Syst. Sci. Int., 47: 806-811.
- Chernousko, F.L., K. Zimmermann, N.N. Bolotnik, S.F. Yatsun and I. Zeidis, 2005. Vibration-driven robots. Proceedings of the Workshop on Adaptive and Intelligent Robots: Present and Future, Volume 1, November 24-26, 2005, Moscow, Russia, pp: 26-31.
- Gear, C.W. and L.R. Petzold, 1984. ODE methods for the solution of differential/algebraic systems. SIAM J. Numer. Anal., 21: 716-728.
- Sooraksa, P. and G. Chen, 1998. Mathematical modeling and fuzzy control of a flexible-link robot arm. Math. Comput. Modell., 27: 73-93.
- Yatsun, S.F., P.A. Bezmen and U.U. Losev, 2008. Mathematical simulation of vibration robot with internal movement bulk. Vibration Systems and Technologies, Kursk, pp: 241-247.